energies

MDPI

*Article*

# Life Cycle Energy Cost Assessment for Pump Units with Various Types of Line-Start Operating Motors Including Cable Losses

**Vadim Kazakbaev [1], Vladimir Prakht [1,*], Vladimir Dmitrievskii [1], Safarbek Oshurbekov [1] and Dmitry Golovanov [2]**

[1] Department of Electrical Engineering and Electric Technology Systems, Ural Federal University, Ekaterinburg 620002, Russia; vadim.kazakbaev@urfu.ru (V.K.); vladimir.dmitrievsky@urfu.ru (V.D.); safarbek.oshurbekov@urfu.ru (S.O.)

[2] Department of Electrical Engineering, University of Nottingham, Nottingham NG7 2RD, UK; dmitry.golovanov@nottingham.ac.uk

* Correspondence: va.prakht@urfu.ru

Received: 11 June 2020; Accepted: 6 July 2020; Published: 9 July 2020


**Abstract:** The paper presents a comparative analysis of life-cycle energy consumption for three different types of 4 kW line-start motors used in a pump unit with throttling: the most widely used induction motor with IE3 efficiency class, line start permanent magnet synchronous motor with IE4 efficiency class and line start synchronous reluctance motor with IE4 efficiency class. The operating cycle for pump units with constant flow is considered for the above-mentioned types of motors taking into account not only the losses in the pump and motor, but also in the power supply cable. It is shown that the line start synchronous reluctance motor without magnets has the highest efficiency over the entire considered loading range. However, its power factor is lower than that of the synchronous motor with magnets and therefore it has more significant losses in power supply cable. Despite this disadvantage, the line-start reluctance motor is a good alternative to widespread induction motor since it allows saving of approximately 4000 euro more than the latter during the 20 years life cycle. It also provides similar savings in comparison to the permanent magnet synchronous motor, but unlike it, it does not have costly rare-earth materials in the rotor.

**Keywords:** centrifugal pump; energy efficiency; induction motor; line-start synchronous motor; synchronous reluctance motor; throttling control

## 1. Introduction

Nowadays, most of the drives with the direct start from the mains power supply utilize induction motors (IM) with aluminium squirrel cage. Typically, IM with casting squirrel cage has a relatively low class of efficiency IE3 [1,2].

Although it is currently acceptable to use the motors with the efficiency class IE3 for industrial applications, according to the EU plans, the efficiency requirements will be increased in the future. For instance, starting from 1st of July 2023, the motors in the EU with the output power greater than 75 kW should comply with the IE4 class of efficiency [3]. Future plans imply the expansion of IE4 requirements to the motors with lower output power (<75 kW) and moving towards the IE5 class of efficiency for high output power motors [4]. In addition, even at the present time, the use of motors of IE4 and IE5 classes can be feasible, due to constantly increasing cost of energy resources and the need to reduce environmental impact [5].

Therefore, further efficiency improvement of IM is necessary in order to comply with upcoming changes in energy efficiency standards. One of the possible ways is to replace the aluminium squirrel

cage with a copper one. However, the latter is more expensive in comparison to the aluminium squirrel cage [2]. For that reason, the IMs with copper squirrel cage are not so widespread for the drives with direct start from the mains power supply.

Recently, the major industrial companies [6,7] have developed synchronous permanent magnet motors with the line start from the mains power supply—so-called line start permanent magnet synchronous motors (LS-PMSM), which comply with the IE4 class efficiency. Such synchronous motors have a squirrel cage type winding on the rotor. This squirrel cage allows starting the motor directly from the mains power supply in asynchronous mode. The rotor accelerates until its frequency gets close to the synchronous frequency. In synchronous mode, the squirrel cage dampens rotor vibrations during sudden changes in load.

There is a number of publications dedicated to the development of LS-PMSM [8–13]. However, LS-PMSM cannot compete with IM contribution to industrial use due to the high cost of the former. Another problem in the manufacturing of LS-PMSM is its technological dependence on rare earth materials suppliers from China. About 95% of the total amount of rare earth raw materials worldwide comes from China [14]. Since this situation is unlikely to change in the foreseeable future, there is always a threat of an unstable change in the price of raw materials for the production of permanent magnets. The already high prices for materials for the production of rare earth magnets can change several times within a few years [14,15].

In addition, the rare earth mineral processing technology is associated with significant environmental damage. It is claimed that the processing of each ton of rare-earth element concentrate results in generation of 1–1.4 t of radioactive waste. Only a small part of the resulting slush contains rare-earth elements and is subsequently extracted for refinement [16].

In view of the above-noted disadvantages of the motors with rare earth magnets, an alternative to the LS-PMSM must be sought. Currently, synchronous reluctance motors (SynRM), which have no magnets and no short-circuited startup winding in the rotor, and are powered by a variable frequency drive (VFD) are the good alternatives to IM [17–21]. They meet the criteria of IE4 energy efficiency [22,23] and IE5 [19,24,25], according to the standard IEC 60034-30-2 «Rotating electrical machines – Part 30-2: Efficiency classes of variable speed AC motors (IE-code)». These kinds of SynRMs were recently launched for production by large industrial companies. [22,26,27].

There are also IE4 energy efficiency class synchronous reluctance motors that are powered directly from the mains power supply, the rotor of which is manufactured with a short-circuited startup winding (line start synchronous reluctance motor, LS-SynRM) [28–31]. These kinds of LS-SynRMs have a higher energy efficiency class than IM as well as approximately the same manufacturing cost [32].

Wide use of energy-efficient LS-SynRMs can lead to a decrease in energy consumption and energy intensity of GDP, as well as lower Greenhouse Gas emissions during electricity generation. The use of energy-efficient LS-SynRM instead of IM will help to achieve the goals stated in the energy and environmental strategies of the European Union (European Green Deal [5]), USA (State Energy Program [33]), Switzerland (supporting Paris Climate Agreement [34]), China (supporting Paris Climate Agreement [35]), Japan (Net Zero Energy Building [36]), South Korea (supporting Paris Climate Agreement [37]) and other countries.

Pump systems consume almost 22% of all electric energy generated throughout the world [38]. Most of the pump drives are powered directly from the mains power supply [39,40]. This suggests the high energy-saving potential of LS-SynRM in pump applications.

A large number of works are dedicated to the comparison of the energy consumption of pumping systems with various types of motors (induction motors, synchronous motors with rare earth permanent magnets, synchronous reluctance motors without magnets). However, all these works are dedicated to pumping systems with motor frequency control using variable frequency drive (VFD) [17,21,41–43].

Energy-saving effect of using various types of motors in pumping systems powered directly from the mains power supply are considered much less frequently. Thus, in [40] the comparison of the energy consumption for LS-PMSM and IM with the direct feed from the mains power supply of classes

IE3 and IE4 in a centrifugal pump with a throttling control is considered. In that work, it was shown that when choosing the motor, it is necessary to take into account not only the energy efficiency class, but also the efficiency under reduced loads.

However, the estimation of the energy-saving effect of LS-SynRM use in pumping systems, and their comparison to IM and LS-PMSM, including the energy losses in power supply cable, has not yet been considered in the literature to the best of our knowledge. The energy losses in the power supply cable depend on the power factor. The power factor should be taken into account due to the increased reactive component of the current, which contributes significantly to the increase of the total current. In [44–46], it is noted that LS-SynRM has a small power factor, which can lead to losses in the power supply cable. Since the motors studied in this article have different values of the power factor, not only their efficiency but also their influence of the power factor on losses in the power supply cable is taken into account when comparing their energy consumption.

In this paper, a comparative assessment of the energy consumption for a low-power pump drive (4 kW) with various types of electric motors is carried out. The following electric motor types are considered: LS-SynRM with energy efficiency class IE4 (Figure 1a), LS-PMSM with energy efficiency class IE4 (Figure 1b) and IM with energy efficiency class IE3 (Figure 1c). All three considered motors have a similar design of the stator. However, their rotor design is different. All the motors have a starter cage on the rotor for the asynchronous startup. However, LS-SynRM has also the magnetic anisotropy of the rotor structure formed by magnetic barriers. Therefore, it enters into synchronous operation after starting. LS-PMSM also goes into synchronous operation due to the synchronizing torque produced by the permanent magnets installed in the rotor. The synchronous motors (LS-SynRM and LS-PMSM) usually have a better efficiency compared to IM due to the reduced rotor losses. Various loading modes of the duty cycle of the pump drive with unregulated rotation speed are taken into account. The costs of electric energy consumption during the pump life-cycle is chosen as the main criterion for comparing the motors.

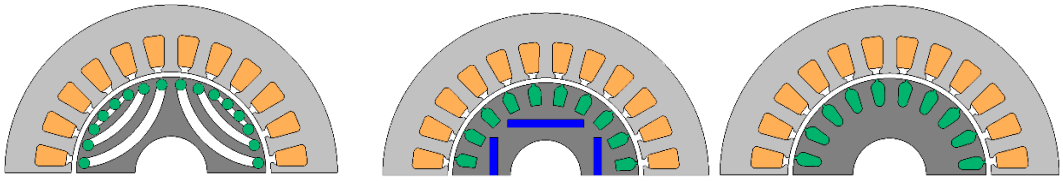


**Figure 1.** Schematic representation of motor geometry: (**a**) line start synchronous reluctance motors (LS-SynRM); (**b**) line start permanent magnet synchronous motors (LS-PMSM); (**c**) induction motors (IM).

It must be highlighted that the analysis presented in this paper is not based on theoretical calculations of motor performances using a modelling software. Instead, an approach to the analysis of energy consumption based on data from manufacturers' datasheets and experimental data is used in the work. For IM and LS-PMSM, the data from manufacturers datasheets are used [47,48]. Since LS-SynRMs of high energy efficiency classes are not yet mass-produced, the experimental data for LS-SynRM are taken from the article [28]. More specifically, the data on the efficiency and power factor of the motors are used in the present analysis. For data processing, polynomial interpolation is applied to the entire load range under consideration. Interpolation of experimental data and other calculations were performed in the MATLAB program and are described in Formulas (1)–(9). The proposed calculation method can be used for choosing the type of electric motor in pumping systems.

## 2. Evaluating Pump Energy Consumption

The mathematical model of pump unit for calculating the energy consumption of a pump drive with various types of the motors is presented below. The schematic representation of the drive of a pump unit with one electric motor, powered directly from the mains power supply, is shown in

Figure 2. The electric motor is fed directly from the mains and is coupled to a centrifugal pump without intermediate mechanical gears. The required motor electrical power $P_{motor\ el}$ depends on the flow $Q$ [39]:

$$P_{motor\ el} = \eta_{\text{motor}} \cdot P_{mech}; \quad (1)$$

$$P_{mech} = \eta_{\text{pump}} \cdot P_{hydr} = \eta_{\text{pump}} \cdot \rho \cdot g \cdot H \cdot Q = f(Q) \quad (2)$$

where $H$—water pressure, is defined from the $H$-$Q$ characteristic of the pump from the catalogue; $g$—acceleration of gravity; ρ—density of a liquid; $P_{hydr}$—hydraulic power of pump; $P_{mech}$—mechanical power of pump, defined from characteristic $P_{mech} = f\ (Q)$ from catalogue; $\eta_{\text{pump}}$—pump efficiency; $\eta_{\text{motor}}$—motor efficiency.

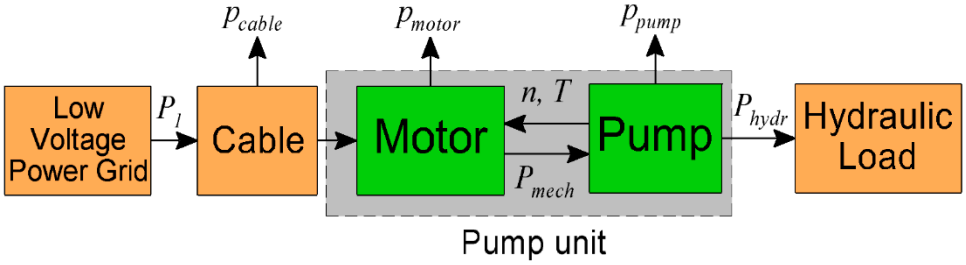


**Figure 2.** Diagram of a single pump unit for fixed-speed operation. In this diagram: $n$, $T$ are the rotational speed and load torque of the motor; $p_{motor}$ is the motor loss; $p_{pump}$ is the pump loss.

In addition to losses in the motor, losses in the power supply cable are also taken into account. The power supply cable electrical loss $p_{cable}$ depends on the active phase resistance of the cable and the value of the motor current [49]:

$$p_{cable} = 3 \cdot R_{cable} \cdot {I_{motor}}^2, \quad (3)$$

where $R_{cable}$—cable phase resistance; $I_{motor}$—motor current.

The motor current is calculated according to formula:

$$I_{motor} = P_{mech} / (\sqrt{3} \cdot V_{motor} \cdot \cos\varphi \cdot \eta_{\text{motor}}), \quad (4)$$

where $V_{motor}$ = 400 V; cosφ and $\eta_{\text{motor}}$—power factor and motor efficiency, according to data from the catalogue.

Considering losses in cable, the electric power $P_1$ consumed from the mains by the pump unit is calculated as:

$$P_1 = \eta_{motor} \cdot P_{mech} + p_{cable}. \quad (5)$$

To calculate the energy consumption of a pump drive, the pump performance characteristics from the manufacturer's datasheets were used [50]. In order to compare the energy consumption of the electric motors as a part of the pump unit when controlling flow by a throttling valve, a centrifugal pump B-NM4 65/25B/B (manufactured by Calpeda S.p.A., Montorso Vicentino, Vicenza, Italy) with the rated power $P_{rate}$ = 4 kW and with rated rotational speed $n$ = 1450 rpm was used [50]. Pump data are shown in Table 1. $Q_{BEP}$ denotes the flow at the best efficient point (BEP), and $H_{BEP}$ denotes the pump head at BEP.

**Table 1.** Published characteristics of the pump from manufacturer.

| Type | Rated Mechanical Power, W | Rate Rotational Speed, rpm | $Q_{BEP}$, $m^3/h$ | $H_{BEP}$, m | Pump Efficiency in BEP, % |
|---|---|---|---|---|---|
| B-NM4 65/25B/B | 4000 | 1450 | 60 | 15.4 | 75.5 |

The calculation was performed for three different four-pole electric motors with the rated power of 4 kW, namely LS-SynRM (a test prototype [28]), LS-PMSM (manufacturer WEG [47]) and IE3 efficiency class induction motor (IM, manufacturer WEG [48]). For the serially produced LS-PMSM and IM, datasheets on their efficiency are used.

There are still no commercially available high-performance LS-SynRMs on the market to the best of our knowledge. ABB Group corporation has announced the launch of IE4 class LS-SynRM [51], however, at the moment of writing this manuscript, these motors are still not available on the market. Therefore, to perform the calculation of LS-SynRM power consumption, the data of the experimental sample described in [28] were used.

Efficiency data for the motors are shown in Tables 2 and 3 and in Figure 3. Current data of the motors are shown in Figure 4. Power factor data of the motors are shown in Figure 5. The motor current can be found based on the efficiency and power factor data using Equation (4).

**Table 2.** Motor characteristics.

| Type of Motor | Rated Mechanical Power, W | Poles | Frame Size | Frame Material | Weight, kg | Rated Voltage, V |
|---|---|---|---|---|---|---|
| LS-SynRM | 4000 | 4 | IEC 112 | No data | No data | 400 |
| LS-PMSM | 4000 | 4 | IEC 112 | Cast iron | 49 | 400 |
| IM | 4000 | 4 | IEC 112 | Cast iron | 42 | 400 |

**Table 3.** Motor characteristics.

| Type of Motor | Motor Efficiency, % | | | Motor Power Factor | | |
|---|---|---|---|---|---|---|
| | 50% Load | 75% Load | 100% Load | 50% Load | 75% Load | 100% Load |
| LS-SynRM | 91.6 | 92.4 | 91.9 | 0.607 | 0.713 | 0.755 |
| LS-PMSM | 89.0 | 91.0 | 91.7 | 0.68 | 0.81 | 0.88 |
| IM | 88.7 | 89.1 | 88.8 | 0.6 | 0.72 | 0.78 |

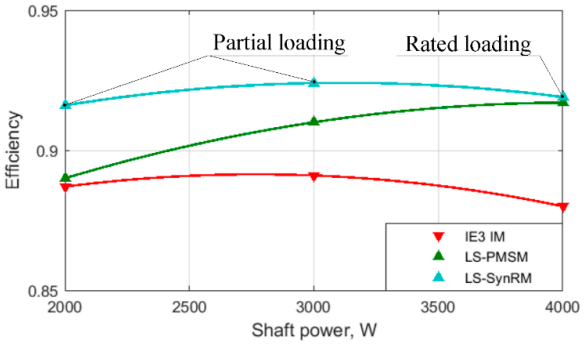


**Figure 3.** Motor efficiency.

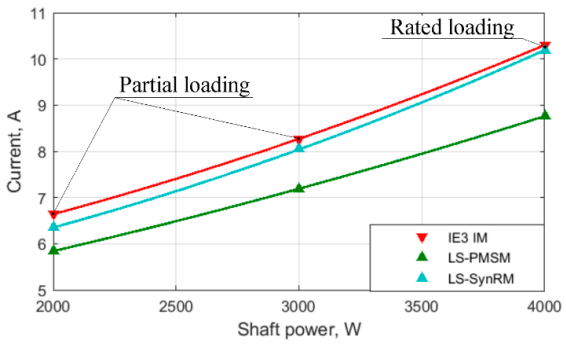


**Figure 4.** Motor current.

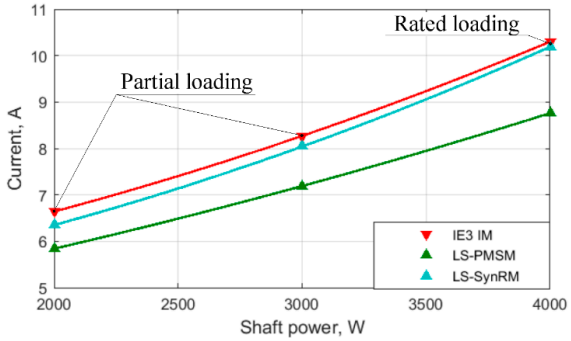


**Figure 5.** Motor power factor.

Note that all three considered motors have approximately the same size and are located in standard casings IEC 112 with mounting dimensions in accordance with IEC standard 60072-1-1991. All data for LS-PMSM and IM are taken from the datasheets of the manufacturer [47,48]. Data for LS-SynRM are taken from the article [28].

In Figures 3–5, the data on motor efficiency, current and power factor are presented. It can be seen that the LS-SynRM has the highest efficiency values in various modes (Figure 3). The rated efficiency of the LS-SynRM is 91.9%. Also, LS-PMSM is more efficient than the traditional IM. According to the data in Table 3, the estimated efficiency of the IM is only 88.8%, while the efficiency of LS-PMSM is significantly higher at 91.7%. Figure 3 also demonstrates that the LS-PMSM efficiency is higher than that of the IM over the entire considered loading range.

The efficiency of the LS-PMSM in the nominal mode is the same as that of the LS-SynRM. However, in partial load modes, the LS-PMSM's efficiency decreases much faster than the one of LS-SynRM. LS-PMSM has the highest power factor. The power factors of IM and LS-SynRM have approximately the same values (0.78 and 0.755, respectively) which are significantly lower than the one for PMSM (0.88). The rate of the power factor decrease with a decrease in load is approximately the same for all studied motors: when the load was decreased from 100% to 50%, the power factor decreased by approximately 0.15.

## 3. Pump Operating Cycle

The operation of the pump unit was considered in the loading points wherein the water flow over the duty cycle changes in accordance with the typical characteristic of fixed-speed pump applications, as shown in reference [52]. In reality, however, even in the case of fixed-speed pumps, the flowrate is very seldom constant. For example, even in a simple pump system when a pump is used to move liquid from one reservoir to another, the duty points vary due to the level of the reservoirs, which means the pump does not operate all the time at the best efficiency. A typical duty cycle of a pump with an approximately constant flowrate described in [52] is characterized by three discrete modes (Figure 6).

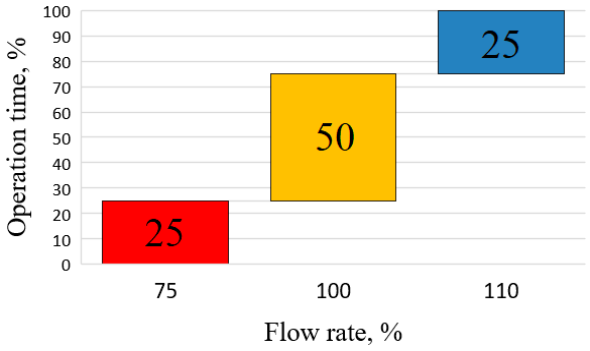


**Figure 6.** Flow-time profile. The numbers in the rectangles indicate the share of the operation time of a loading point.

An electric motor is connected directly to the mains power supply. Therefore, the flow $Q$ of the pump is adjusted using a throttle. In this case, the water pressure changes in accordance with the $Q$-$H$ curve of the pump, and the operating point is the intersection point of the pump characteristic (red line in Figure 7a) and the hydraulic system characteristic (blue, green and emerald lines in Figure 7a). Figure 7a shows the interpolation results of the $Q$-$H$ characteristic of the selected pump according to manufacturer data [50].

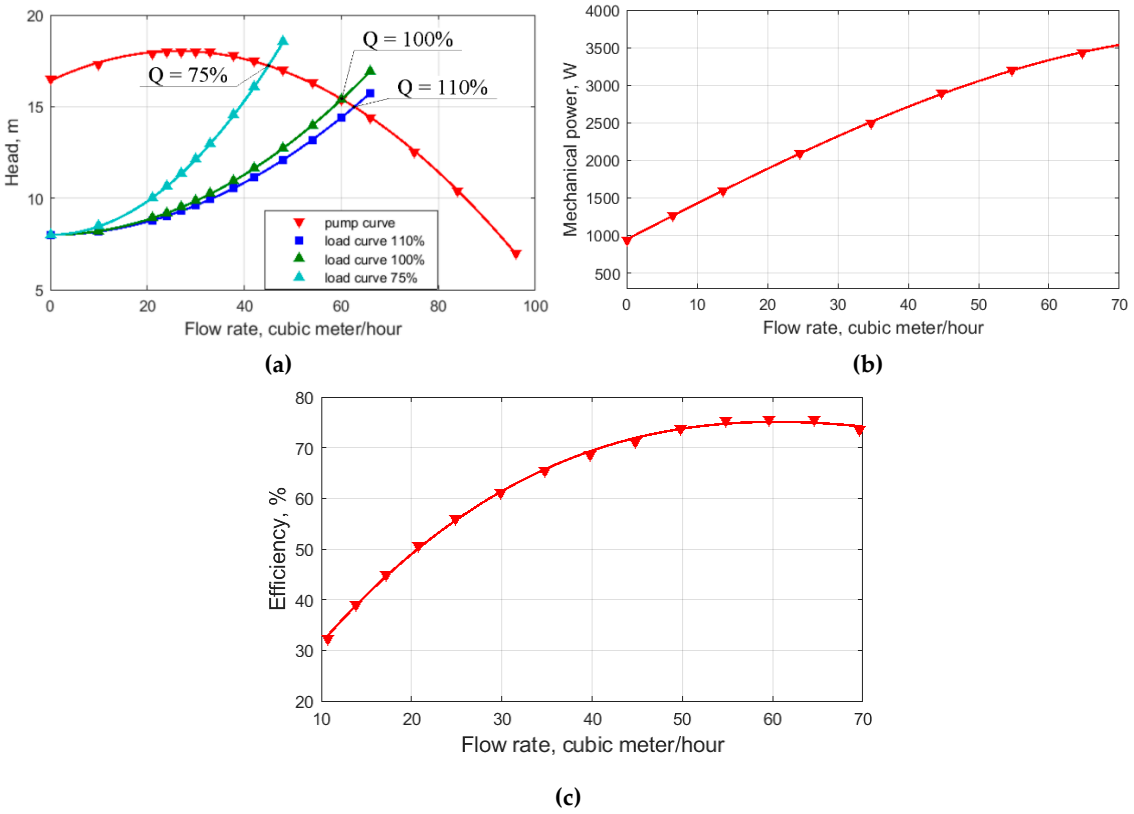


**Figure 7.** Pump performances: (**a**) $Q$-$H$ curve; (**b**) pump mechanical power; (**c**) pump efficiency.

The mechanical (input) power curve of the pump as a function of the flow is reported by the pump manufacturer (Figure 7b). The pump power was determined from the curve in three operation modes (75%, 100% and 110% of the pump flow). The flow corresponding to 100% of the maximum flow in the pump operating cycle was determined based on the pump efficiency curve (Figure 7c) [50], corresponding to maximum efficiency (best efficiency point: $Q = 60\text{m}^3/\text{h}$, $\eta_{\text{pump}} = 0.755$).

The efficiencies of the electric motors (Table 2) at the four operation modes of the pump unit were determined using polynomial interpolation of their specification data.

The obtained efficiency values are provided in Table 4, which also shows the following values for each operating mode: the flow, the pump head, and the mechanical output power of the electric motors as percentages of the rated output.

**Table 4.** Characteristics of pump duty cycle.

| $Q$, % | $Q$, m$^3$/h | $H$, m | $P_{mech}$, W | $T$, N·m | $\eta_{\text{pump}}$, % | $\eta_{\text{motor}}$, % | | |
|---|---|---|---|---|---|---|---|---|
| | | | | | | LS-SynRM | LS-PMSM | IM |
| 110 | 66 | 14.4 | 3453 | 22.0 | 75 | 0.924 | 0.915 | 0.89 |
| 100 | 60 | 15.4 | 3335 | 21.2 | 75.5 | 0.925 | 0.914 | 0.891 |
| 75 | 45 | 17.25 | 2962 | 18.9 | 71.4 | 0.925 | 0.909 | 0.891 |

## 4. Cable Losses Depending on Motor Power Factor

An important energy parameter for a motor with a feed from the mains power supply is not only the efficiency, but also the power factor, because the reactive current fed to a motor flows not only through its winding, but also through a network of elements from which a motor receives power [53] causing additional losses. Since the considered motors have different power factors and total currents (see Figure 4 and Table 5), it is also necessary to evaluate the influence of this factor on the cost of electricity for the consumer.

**Table 5.** Motor current at three points of the duty cycle for various pump modes.

| $Q$, % | $P_{mech}$, W | $I_{motor}$, A | | |
|---|---|---|---|---|
| | | **LS-SynRM** | **LS-PMSM** | **IM** |
| 110 | 3453 | 7.33 | 6.42 | 7.42 |
| 100 | 3335 | 7.12 | 6.27 | 7.23 |
| 75 | 2962 | 6.51 | 5.84 | 6.69 |

Let us have a look at the simplest case when a pump is connected directly to a three-phase 400 V network. In this case, if we want to consider cable losses, we need to take into account the magnitude of the motor current too. For industry, the typical cable length for connecting low-voltage power equipment is about 100 m [54]. In low-power electrical systems with a current load of up to 15A, cables with a cross section of 1.5 mm$^2$ are typically used [55]. The specific resistance of one phase of a copper cable with these parameters is approximately $\rho_{\text{cable}}$ = 12.6 Ohm/km. When performing calculations for the stranded cables of a small cross section, the reactance is usually neglected. We assume that the motor is powered via a typical cable of 100 m length ($l_{cable}$ = 100 m). The phase resistance of such a cable will be $R_{cable} = l_{cable} \cdot \rho_{\text{cable}} = 0.1 \cdot 12.6 = 1.26$ Ohm. Losses in the cable are calculated from (3). The results of interpolation of motor current values for various studied pump modes are presented in Table 5.

Table 6 presents the results of the calculation of losses in the cable according to Formula (3), as well as the values of the losses in the motor, according to the data in Table 4.

**Table 6.** Losses in motor and cable at three points of the duty cycle for various pump modes.

| $Q$, % | $P_{mech}$, W | $p_{motor}$, W | | | $p_{cable}$, W | | |
|---|---|---|---|---|---|---|---|
| | | **LS-SynRM** | **LS-PMSM** | **IM** | **LS-SynRM** | **LS-PMSM** | **IM** |
| 110 | 3453 | 283.6 | 320.8 | 426.8 | 203.0 | 155.6 | 208.0 |
| 100 | 3335 | 272.4 | 313.8 | 408.0 | 191.8 | 148.6 | 197.7 |
| 75 | 2962 | 241.9 | 296.6 | 362.4 | 160.0 | 128.8 | 169.4 |

In accordance with the assumptions made, the estimated losses in cable are comparable with the ones in the motor (Table 6). At the same time, the cable losses for LS-PMSM are lower by approximately 25% than for LS-SynRM and IM. The main reason of the reduced cable losses for LS-PMSM is its reduced total current due to its higher power factor, according to Equations (3) and (4). These results confirm the importance of the power factor increase for reduction of the energy consumption of the line-start motors.

## 5. Electric Energy Consumption Results and Discussion

Using the results obtained in the previous sections, we compared the energy consumption of the pump drive with various motors: LS-SynRM, LS-PMSM and IM motor. The daily energy consumption

for each electric motor over a full duty cycle of the pump unit in accordance with the corresponding load profile (Figure 6) is determined as:

$$E_{day} = t_{\Sigma} \cdot \sum_{i=1}^{3} (P_{1\,i} \cdot t_i / t_{\Sigma}). \quad (6)$$

where $i = 1 \ldots 3$ is the number of a loading point; $P_{1\,i}$ is the eclectic power $P_1$ in a loading point; $t_i/t_{\Sigma}$ is the share of the operation time of a loading point.

For the year-round operation of the pump unit, the annual energy consumption was calculated as follows:

$$E_{year} = E_d \cdot 365. \quad (7)$$

The cost of electricity consumed (in Euro), considering the applied grid tariffs $GT = 0.2036$ €/kW·h for non-household consumers [56] for Germany in the second half of 2019, was calculated as follows:

$$C_{year} = E_y \cdot GT. \quad (8)$$

The whole life cycle of pump units is usually about 20 years [57,58]. The energy cost for the lifespan of $n = 20$ years is assessed without taking into account the maintenance costs and the initial cost of the motors since the market cost of the motors depends on many factors and this was beyond of the topic of the present paper. Furthermore, the pump lifetime expenses often consist mostly of the energy cost (>50–60%) [57,58]. The net present value (NPV) of the life-cycle cost was calculated as follows:

$$C_{LCC} = \sum_{i=1}^{n} \left( C_{year} / [1 + (y - p)]^i \right), \quad (9)$$

where $y$— interest rate ($y = 0.04$); $p$—expected annual inflation ($p = 0.02$); $n$—lifetime of the pump unit ($n = 20$ years) [58].

The results of calculations based on (1)–(9) excluding and including cable losses are presented in Tables 7 and 8, respectively. Figure 8 presents calculated values of life cycle energy cost $C_{LCC}$ for both cases. The energy savings of LS-SynRM and LS-PMSM is assessed in relation to the induction motor.

**Table 7.** Calculation of energy consumption excluding cable losses.

| | $t_i/t_{\Sigma}$, % | LS-SynRM | LS-PMSM | IM |
|---|---|---|---|---|
| $P_1$, W | 25 | 3736.7 | 3773.9 | 3879.9 |
| | 50 | 3607.3 | 3648.8 | 3742.9 |
| | 25 | 3204.5 | 3259.2 | 3325.0 |
| $E_{day}$, kW·hour | | 84.9 | 86.0 | 88.1 |
| $E_{year}$, kW·hour | | 31,001 | 31,384 | 32,173 |
| Annual energy savings, kW·hour | | 1171 | 789 | – |
| Annual energy savings, % | | 3.65 | 2.45 | – |
| Cost savings, € (per year) | | 238.5 | 160.6 | – |
| Cost savings, € (per 20 years) | | 3900 | 2626 | – |
| Life cycle energy cost $C_{LCC}$, € (20 years) | | 103,208 | 104,482 | 107,108 |

**Table 8.** Calculation of energy consumption including cable losses.

| | $t_i/t_\Sigma$, % | LS-SynRM | LS-PMSM | IM |
|---|---|---|---|---|
| $P_1$, W | 25 | 3939.7 | 3929.5 | 4087.9 |
| | 50 | 3799.1 | 3797.3 | 3940.7 |
| | 25 | 3364.5 | 3387.9 | 3494.4 |
| $E_{day}$, kW·hour | | 89.4 | 89.4 | 92.8 |
| $E_{year}$, kW·hour | | 32,636 | 32,658 | 33,865 |
| Annual energy savings, kW·hour | | 1228.9 | 1207.6 | – |
| Annual energy savings, % | | 3.6 | 3.6 | – |
| Cost savings, € (per year) | | 250.2 | 245.9 | – |
| Cost savings, € (per 20 years) | | 4181 | 4020 | – |
| Life cycle energy cost $C_{LCC}$, € (20 years) | | 108,651 | 108,722 | 112,742 |

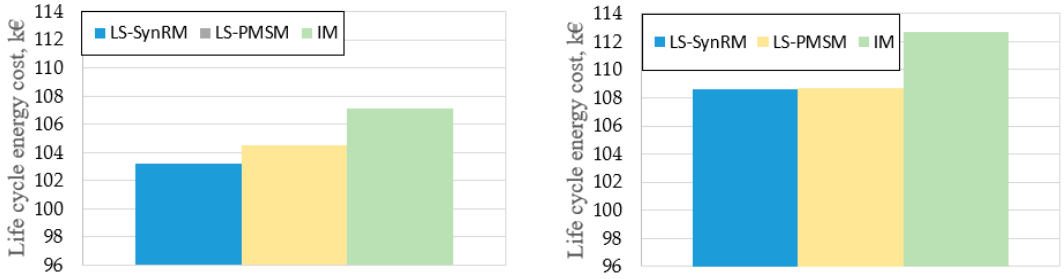


**Figure 8.** Life cycle energy cost (20 years) using various motor types: (**a**) without considering cable loss; (**b**) considering cable loss.

From Tables 7 and 8 and Figure 8 we can see that without taking into account the cable losses, LS-SynRM provides the lowest energy consumption ($E_{day}$ = 84.9 and $E_{year}$ = 31,001 kW·hour) which is 3.65% more annual energy saving than for IM. For the LS-PMSM and IM the daily energy consumption values are 86.0 and 88.1 kW hour, respectively, and their annual energy consumption is 31,384 and 32,173 kW hour, respectively. The annual cost saving for LS-PMSM is 2.45% higher than for IM. When the cable losses are taken into account the energy savings in relation to IM of both LS-SynRM and LS-PMSM raise to 3.6%.

The life cycle energy cost for 20 years of use is estimated in euros and is 108,651, 108,722 and 112,742 € including cable losses for LS-SynRM, LS-PMSM and IM, respectively. It can be seen that for LS-SynRM, the life cycle savings in energy costs against the IM excluding and including cable losses are relatively similar 3900 € and 4181 €, respectively. In case of using LS-PMSM, the savings increase almost double from 2626 € to 4020 € when the cable losses were taken into account. Thus, before making a choice of particular motor type and calculating the payback period, it is necessary to take into account not only the efficiency of the motors, but also the power factor and its effect on cable losses, as this can significantly affect the results of the feasibility study.

However, as we have already mentioned above, LS-PMSMs have a higher cost compared to IM and LS-SynRM due to the use of expensive rare-earth magnets in its design. In addition, the rare-earth elements processing from raw ore is associated with significant environmental damage [16]. Therefore, the LS-SynRM, which does not have permanent magnets and has a comparable cost to IM, is the most attractive pumping system in terms of energy saving even taking into account cable losses.

## 6. Conclusions

The present paper provides a comparative analysis of the energy consumption of electric motors of various types (LS-SynRM, LS-PMSM and IM) used as part of a 4 kW fixed-speed pump unit with throttle control. The comparison takes into account not only the efficiency of the motors at different pump loads, but also the effect of the motor power factor on cable losses in the power supply line.

It is shown that the life cycle energy cost savings for LS-SynRM compared to IM was 3900 € excluding cable losses. For LS-PMSM this number was 2626 €. However, when taking into account the cable losses, affected by the power factor and the total current of the motor, the savings for both LS-SynRM and LS-PMSM are almost the same: 4181 € and 4020 €, respectively.

Therefore, when selecting the motor type and calculating the payback period, it is necessary to take into account not only the efficiency of the motors, but also the motor power factor and its impact on the cable losses, as this can significantly affect the results of the feasibility study.

Thus, the use of LS-SynRM in the considered pump application provides lower cost of motor manufacturing and environmental friendliness, compared to LS-PMSM, and energy savings of more than 4000 € during the life cycle, compared to IM.

Based on this study, LS-SynRM can be suggested as the best alternative for the considered pump application since having the lowest energy consumption. In addition, LS-SynRM has the manufacturing cost comparable to IMs, while the cost of LS-PMSM is significantly higher, due to the presence of permanent magnets, the extraction of which is harmful to the environment.

The proposed method can be applied in the analysis of the energy consumption of other motor types used in pump stations, for example, line-start permanent magnet assisted synchronous reluctance motors (LS-PMaSynRM).

**Author Contributions:** Conceptual approach, V.K. and V.P.; data curation, D.G., S.O., and V.K.; software, S.O. and V.K.; calculations and modelling, S.O., V.D., V.K. and V.P.; writing of original draft, D.G., S.O., V.D., V.K. and V.P.; visualization, D.G., and V.K.; review and editing, D.G., S.O., V.D., V.K. and V.P. All authors have read and agreed to the published version of the manuscript.

**Funding:** This research received no external funding.

**Acknowledgments:** The authors thank the editors and reviewers for careful reading and constructive comments.

**Conflicts of Interest:** The authors declare no conflict of interest.

## References

1. ABB Group. Process Performance IE3 Aluminum Motors, 50/60 Hz. The Product Range for Global Customers, Product Note. 2017. Available online: https://www.baldor.com/mvc/DownloadCenter/Files/9AKK107020 (accessed on 9 June 2020).
2. Almeida, A.; Ferreira, F.; Baoming, G. Beyond Induction Motors—Technology Trends to Move Up Efficiency. *IEEE Trans. Ind. Appl.* **2014**, *50*, 2103–2114. [CrossRef]
3. Commission Regulation (EU) 2019/1781 of 1 October 2019 Laying Down Ecodesign Requirements for Electric Motors and Variable Speed Drives Pursuant to Directive 2009/125/EC of the European Parliament and of the Council, Amending Regulation (EC) No 641/2009 with Regard to Ecodesign Requirements for Glandless Standalone Circulators and Glandless Circulators Integrated in Products and Repealing Commission Regulation (EC) No 640/2009, Document 32019R1781. Available online: https://eur-lex.europa.eu/legal-content/EN/TXT/PDF/?uri=CELEX:32019R1781&from=EN (accessed on 9 June 2020).
4. Doppelbauer, M. Update on IEC motor and converter standards. In Proceedings of the 6th International Motor Summit for Energy Efficiency powered by Impact Energy, Motor Summit 2016, Zurich, Switzerland, 11–12 October 2016.
5. Annex to the Communication from the Commission to the European Parliament, the European Council, the Council, the European Economic and Social Committee and the Committee of the Regions, The European Green Deal, Brussels, 11.12.2019, COM(2019) 640 Final. Available online: https://ec.europa.eu/info/sites/info/files/european-green-deal-communication-annex-roadmap_en.pdf (accessed on 9 June 2020).

6. WQuattro, Super Premium Efficiency Motor. WEG Group, Catalogue, Code 50025713, Revision 3 July 2017. Available online: https://static.weg.net/medias/downloadcenter/h01/hfc/WEG-w22-quattro-european-market-50025713-brochure-english-web.pdf (accessed on 9 June 2020).
7. Synchro Vert IE4 Super Premium Efficiency Motors, Bharat Bijlee, Catalogue. Available online: https://www.bharatbijlee.com/media/14228/synchrovert_catalogue.pdf (accessed on 5 May 2020).
8. Ismagilov, F.; Vavilov, V.; Gusakov, D. Line-Start Permanent Magnet Synchronous Motor for Aerospace Application. In Proceedings of the 2018 IEEE International Conference on Electrical Systems for Aircraft, Railway, Ship Propulsion and Road Vehicles and International Transportation Electrification Conference (ESARS-ITEC 2018), Nottingham, UK, 7–9 November 2018; pp. 1–5. [CrossRef]
9. Sorgdrager, J.; Wang, R.-J.; Grobler, A. Multi-Objective Design of a Line-Start PM Motor Using the Taguchi Method. *IEEE Trans. Ind. Appl.* **2018**, *54*, 4167–4176. [CrossRef]
10. Kurihara, K.; Rahman, M. High-Efficiency Line-Start Interior Permanent-Magnet Synchronous Motors. *IEEE Trans. Ind. Appl.* **2004**, *40*, 789–796. [CrossRef]
11. Azari, M.; Mirsalim, M. Line-start permanent-magnet motor synchronisation capability improvement using slotted solid rotor. *IET Electr. Power Appl.* **2013**, *7*, 462–469. [CrossRef]
12. Ghahfarokhi, M.; Aliabad, A.; Boroujeni, S.; Amiri, E.; Faradonbeh, V. Analytical modelling and optimization of line start LSPM synchronous motors. *IET Electr. Power Appl.* **2020**, *14*, 398–408. [CrossRef]
13. Sethupathi, P.; Senthilnathan, N. Comparative analysis of line-start permanent magnet synchronous motor and squirrel cage induction motor under customary power quality indices. *Electr. Eng.* **2020**, 1–11. [CrossRef]
14. Dent, P. Rare earth elements and permanent magnets. *J. Appl. Phys.* **2012**, *111*, 07A721. [CrossRef]
15. Goss, J.; Popescu, M.; Staton, D. A Comparison of an Interior Permanent Magnet and Copper Rotor Induction Motor in a Hybrid Electric Vehicle Application. In Proceedings of the IEEE International Electric Machines & Drives Conference, EMDC, Chicago, IL, USA, 12–15 May 2013; pp. 12–15. [CrossRef]
16. Lima, I.; Filho, W. *Rare Earth Industry*; Elsevier: Amsterdam, The Netherlands, 2015.
17. Kazakbaev, V.; Prakht, V.; Dmitrievskii, V.; Ibrahim, M.N.; Oshurbekov, S.; Sarapulov, S. Efficiency Analysis of Low Electric Power Drives Employing Induction and Synchronous Reluctance Motors in Pump Applications. *Energies* **2019**, *12*, 1144. [CrossRef]
18. Moghaddam, R.; Magnussen, F.; Sadarangani, C. Theoretical and Experimental Reevaluation of Synchronous Reluctance Machine. *IEEE Trans. Ind. Electron.* **2010**, *57*, 6–13. [CrossRef]
19. Kabir, M.; Husain, I. Application of a Multilayer AC Winding to Design Synchronous Reluctance Motors. *IEEE Trans. Ind. Appl.* **2018**, *54*, 5941–5953. [CrossRef]
20. Pellegrino, G.; Cupertino, F.; Gerada, C. Automatic Design of Synchronous Reluctance Motors Focusing on Barrier Shape Optimization. *IEEE Trans. Ind. Appl.* **2015**, *51*, 1465–1474. [CrossRef]
21. Kazakbaev, V.; Prakht, V.; Dmitrievskii, V.; Sarapulov, S.; Askerov, D. Comparison of power consumption of synchronous reluctance and induction motor drives in a 0.75 kW pump unit. In Proceedings of the 2017 International Siberian Conference on Control and Communications (SIBCON), Kazakhstan, Astana, 29–30 June 2017; pp. 1–6. [CrossRef]
22. ABB Group. Low Voltage IE4 Synchronous Reluctance Motor and Drive Package for Pump and Fan Applications, Catalogue. 2013. Available online: https://library.e.abb.com/public/21ee11b9fddfa677c1257bd500219300/Catalog_IE4_SynRM_EN_06-2013_9AKK105828_lowres.pdf (accessed on 9 June 2020).
23. Jia, S.; Zhang, P.; Liang, D.; Dai, M.; Liu, J. Design of IE4 Level Synchronous Reluctance Machines with Different Number of Poles. In Proceedings of the 2019 22nd International Conference on Electrical Machines and Systems (ICEMS), Harbin, China, 11–14 August 2019; pp. 1–5. [CrossRef]
24. Dmitriveskii, V.; Prakht, V.; Kazakbaev, V. IE5 Energy-Efficiency Class Synchronous Reluctance Motor with Fractional Slot Winding. *IEEE Trans. Ind. Appl.* **2019**, *55*, 4676–4684. [CrossRef]
25. Dmitrievskii, V.; Prakht, V.; Kazakbaev, V.; Oshurbekov, S.; Sokolov, I. Developing ultra premium efficiency (IE5 class) magnet-free synchronous reluctance motor. In Proceedings of the 2016 6th International Electric Drives Production Conference (EDPC), Nuremberg, Germany, 30 November–1 December 2016; pp. 2–7. [CrossRef]
26. REEL SuPremE®–The IE5* Magnet-Free Synchronous Reluctance Motor, KSB Company, Catalogue. 2019. Available online: https://www.ksb.com/blob/199782/10a90edea2eca4cb28afab3076d43df3/reel-supreme-motor-brochure-en-dow-data.pdf (accessed on 8 July 2020).

27. SIMOTICS Reluctance Motors with SINAMICS Converters, Siemens AG, Catalog. 2015. Available online: https://www.asberg.ru/upload/iblock/919/9195144e44c436fd94d723be0813ecfe.pdf (accessed on 9 June 2020).
28. Kersten, A.; Liu, Y.; Pehrman, D.; Thiringer, T. Rotor Design of Line-Start Synchronous Reluctance Machine with Round Bars. *IEEE Trans. Ind. Appl.* **2019**, *55*. [CrossRef]
29. Liu, H.; Lee, J. Optimum Design of an IE4 Line-Start Synchronous Reluctance Motor Considering Manufacturing Process Loss Effect. *IEEE Trans. Ind. Electron.* **2018**, *65*, 3104–3114. [CrossRef]
30. Kärkkäinen, H.; Aarniovuori, L.; Niemelä, M.; Pyrhönen, J.; Kolehmainen, J.; Känsäkangas, T.; Ikäheimo, J. Direct-On-Line Synchronous Reluctance Motor Efficiency Verification with Calorimetric Measurements. In Proceedings of the 2018 XIII International Conference on Electrical Machines (ICEM), Alexandroupoli, Greece, 3–6 September 2018; pp. 171–177. [CrossRef]
31. Hu, Y.; Chen, B.; Xiao, Y.; Shi, J.; Li, L. Study on the Influence of Design and Optimization of Rotor Bars on Parameters of a Line-Start Synchronous Reluctance Motor. *IEEE Trans. Ind. Appl.* **2020**, *56*, 1368–1376. [CrossRef]
32. Gamba, M.; Armando, E.; Pellegrino, G.; Vagati, A.; Janjic, B.; Schaab, J. Line-start synchronous reluctance motors: Design guidelines and testing via active inertia emulation. In Proceedings of the 2015 IEEE Energy Conversion Congress and Exposition (ECCE), Montreal, QC, Canada, 20–24 September 2015; pp. 4820–4827. [CrossRef]
33. Weatherization and Intergovernmental Programs Office, About the State Energy Program. Available online: https://www.energy.gov/eere/wipo/about-state-energy-program (accessed on 9 June 2020).
34. Federal Council Aims for a Climate-Neutral Switzerland by 2050. Available online: https://www.admin.ch/gov/en/start/documentation/media-releases.msg-id-76206.html (accessed on 9 June 2020).
35. Hopes of Limiting Global Warming? China and the Paris. Agreement on Climate Change. Available online: https://journals.openedition.org/chinaperspectives/6924?file=1 (accessed on 9 June 2020).
36. Japan Net Zero Energy Building Roadmap. Available online: http://www.nzeb.in/wp-content/uploads/2015/09/Japan-NZEB-Roadmap.pdf (accessed on 9 June 2020).
37. Ha, S.; Tae, S.; Kim, R. A Study on the Limitations of South Korea's National Roadmap for Greenhouse Gas Reduction by 2030 and Suggestions for Improvement. *Sustainability* **2019**, *11*, 3969. [CrossRef]
38. Shankar, V.; Umashankar, S.; Paramasivam, S.; Hanigovszki, N. A comprehensive review on energy efficiency enhancement initiatives in centrifugal pumping system. *Appl. Energy* **2016**, *181*, 495–513. [CrossRef]
39. Stoffel, B. Assessing the Energy Efficiency of Pumps and Pump Units. In *Background and Methodology*; Elsevier: Amsterdam, The Netherlands, 2015.
40. Goman, V.; Oshurbekov, S.; Kazakbaev, V.; Prakht, V.; Dmitrievskii, V. Energy Efficiency Analysis of Fixed-Speed Pump Drives with Various Types of Motors. *Appl. Sci.* **2019**, *9*, 5295. [CrossRef]
41. Ahonen, T.; Orozco, S.; Ahola, J.; Tolvanen, J. Effect of electric motor efficiency and sizing on the energy efficiency in pumping systems. In Proceedings of the 2016 18th European Conference on Power Electronics and Applications (EPE'16 ECCE Europe), Karlsruhe, Germany, 5–9 September 2016; pp. 1–9. [CrossRef]
42. Rhyn, P.; Pretorius, J. Utilising high and premium efficiency three phase motors with VFDs in a public water supply system. In Proceedings of the 2015 IEEE 5th International Conference on Power Engineering, Energy and Electrical Drives (POWERENG), Riga, Latvia, 11–13 May 2015; pp. 497–502. [CrossRef]
43. Brinner, T.; McCoy, R.; Kopecky, T. Induction versus Permanent-Magnet Motors for Electric Submersible Pump Field and Laboratory Comparisons. *IEEE Trans. Ind. Appl.* **2014**, *50*, 174–181. [CrossRef]
44. Ogunjuyigbe, A.; Jimoh, A.; Nicolae, D.; Obe, E. Analysis of synchronous reluctance machine with magnetically coupled three-phase windings and reactive power compensation. *IET Electr. Power Appl.* **2010**, *4*, 291–303. [CrossRef]
45. Obe, E. Steady-state performance of a line-start synchronous reluctance motor with capacitive assistance. *Electr. Power Syst. Res.* **2010**, *80*, 1240–1246. [CrossRef]
46. Gamba, M.; Pellegrino, G.; Vagati, A.; Villata, F. Design of a line-start synchronous reluctance motor. In Proceedings of the 2013 International Electric Machines & Drives Conference, Chicago, IL, USA, 12–15 May 2013; pp. 648–655. [CrossRef]
47. Wquattro 4 kW 4P 112M 3Ph 400/690 V 50 Hz IC411-TEFC-B3T. Product Details. Available online: https://www.weg.net/catalog/weg/RS/en/Electric-Motors/Special-Application-Motors/Permanent-Magnet-Motors/Line-Start-PM-Motors/Wquattro-4-kW-4P-112M-3Ph-400-690-V-50-Hz-IC411---TEFC---B3T/p/13009391 (accessed on 9 June 2020).

48. W22 IE3 4 kW 4P 112M 3Ph 220-240/380-415//460 V 50 Hz IC411-TEFC-B14T. Product Details. Available online: https://www.weg.net/catalog/weg/RS/en/Electric-Motors/Low-Voltage-IEC-Motors/General-Purpose-ODP-TEFC/Cast-Iron-TEFC-General-Purpose/W22---Cast-Iron-TEFC-General-Purpose/W22-IE3/W22-IE3-4-kW-4P-112M-3Ph-220-240-380-415-460-V-50-Hz-IC411---TEFC---B14T/p/14640586 (accessed on 9 June 2020).
49. Matine, A.; Bonnard, C.-H.; Blavette, A.; Bourguet, S.; Rongère, F.; Kovaltchouk, T.; Schaeffer, E. Optimal sizing of submarine cables from an electro-thermal perspective. In Proceedings of the European Wave and Tidal, Conference (EWTEC), Cork, Ireland, 27 August–1 September 2017; Available online: https://hal.archives-ouvertes.fr/hal-01754060 (accessed on 9 June 2020).
50. NM; NMS. Close Coupled Centrifugal Pumps with Flanged Connections; Catalogue; Calpeda. 2018. Available online: https://www.calpeda.com/system/pdf/catalogue_en_50hz.pdf (accessed on 5 May 2020).
51. IE4 DOLSynRM Concept Introduction, SynRM Benefits Available for Fixed Speed Applications. Tailored High Efficiency Motors for OEMs, Document Number: 9AKK106542 EN 04-2015. Available online: https://search.abb.com/library/Download.aspx?DocumentID=9AKK106542&LanguageCode=en&DocumentPartId=&Action=Launch (accessed on 9 June 2020).
52. Extended Product Approach for Pumps, Europump. 2014. Available online: http://europump.net/uploads/Extended%20Product%20Approach%20for%20Pumps%20-%20A%20Europump%20guide%20(27OCT2014).pdf (accessed on 9 June 2020).
53. Zhou, J.-H.; Chen, C.; Zhang, X.-W.; Chen, Y.-A. Reducing voltage energy-saving control method of induction motor. In Proceedings of the 2013 International Conference on Electrical Machines and Systems (ICEMS), Busan, Korea, 26–29 October 2013; pp. 2159–2162. [CrossRef]
54. Kirar, M.; Aginhotri, G. Cable sizing and effects of cable length on dynamic performance of induction motor. In Proceedings of the 2012 IEEE Fifth Power India Conference, Murthal, India, 19–22 December 2012; pp. 1–6. [CrossRef]
55. *Electrical Installations in Buildings—Part 5–52: Selection and Erection of Electrical Equipment—Wiring Systems, Is the IEC Standard Governing Cable Sizing*; IEC 60364-5-52; IEC: Geneva, Switzerland, 2009; Available online: https://webstore.iec.ch/publication/1878 (accessed on 8 July 2020).
56. Eurostat Data for the Industrial Consumers in Germany. Available online: http://ec.europa.eu/eurostat/statistics-explained/index.php/Electricity_price_statistics#Electricity_prices_for_industrial_consumers (accessed on 9 June 2020).
57. *Pump Life Cycle Costs: A Guide to LCC Analysis for Pumping Systems, Executive Summary*; Hydraulic Institute: Parsippany, NJ, USA; Europump: Brussels, Belgium; Office of Industrial Technologies Energy Efficiency and Renewable Energy, U.S. Department of Energy: Washington, DC, USA, 2001; pp. 1–19. Available online: https://www.energy.gov/sites/prod/files/2014/05/f16/pumplcc_1001.pdf (accessed on 8 July 2020).
58. Waghmode, L.; Sahasrabudhe, A. A comparative study of life cycle cost analysis of pumps. In Proceedings of the ASME 2010 International Design Engineering Technical Conferences and Computers and Information in Engineering Conference (ASME 2010), Montreal, QC, Canada, 15–18 August 2010; pp. 491–500. [CrossRef]